SATURABLE ABSOPTION DYNAMICS OF DODCI IN CW FEMTOSECOND DYE LASERS

A.Penzkofer and W. Bäumler
Naturwissenschaftliche Fakultät II - Physik, Universität Regensburg,
Universitätsstraße 31, D-W-8400 Regensburg, Fed. Rep. Germany

The dye DODCI (3,3'-diethyloxadicarbocyanine iodide) is the most widely used saturable dye of cw passive mode-locked or hybrid mode-locked rhodamine 6G femtosecond dye lasers. The saturable absorption dynamics of DODCI is complicated by the presence of two spectroscopic different isomers, the N-isomer and the P-isomer. Light excitation of DODCI leads to P-isomer accumulation. The saturable absorption dynamics of DODCI involves the saturable absorption of the N-isomers and the P-isomers and the N-isomer P-isomer photoisomerization dynamics. The N-isomer and P-isomer transitions may be reduced to three-level systems with fast intraband relaxation (fast partial absorption recovery time $\tau_{rec} \approx 1ps$) and slow $S_1 - S_0$ interband relaxation (final absorption recovery time $\tau_A \approx 1.3ns$). The fast partial absorption recovery of DODCI is necessary for the background suppression in the build-up of femtosecond pulses in the laser. The slow final absorption recovery time facilitates a low mode-locking threshold because of the low steady-state saturation intensity of the absorber bleaching.

1. Introduction

The cyanine dye DODCI (3,3'-diethyloxadicarbocyanine iodide, structural formula is shown in Fig.1)[1] forms two spectroscopic different isomers, the cis,cis-1,5-DODCI N-isomer and the all-trans DODCI P-isomer[2]. The dye is widely used as saturable absorber in mode-locked dye lasers, especially rhodamine 6G dye lasers[3-7]. In femtosecond rhodamine 6G – DODCI dye lasers pulse durations down to 19 fs were obtained using a prism quadruple balanced ring colliding-pulse mode-locked (CPM) resonator arrangement[8] , and pulse duration down to 38 fs were obtained with a prism pair balanced linear hybrid mode-locked arrangement[9] .

In this paper absorption and emission spectroscopic data of DODCI in the solvent ethylene glycol are given, results of the photoisomerization dynamics studies are summarized, and the saturable absorption dynamics of the N-isomers and P-isomers is described. The saturable absorber action of DODCI in a cw pumped passive mode-locked linear femtosecond rhodamine 6G – DODCI laser is reviewed.

2. Absorption and Emission Spectroscopic Results

The absorption spectrum of DODCI has a shoulder in the long wavelength region of the $S_0 - S_1$ transition[10]. This absorption shoulder was identified as the $S_0 - S_1$ absorption of thermally populated P-isomers[10,11]. Temperature dependent measurements of the absorption spectra allowed the determination of the S_0-level energy position of the P-isomer

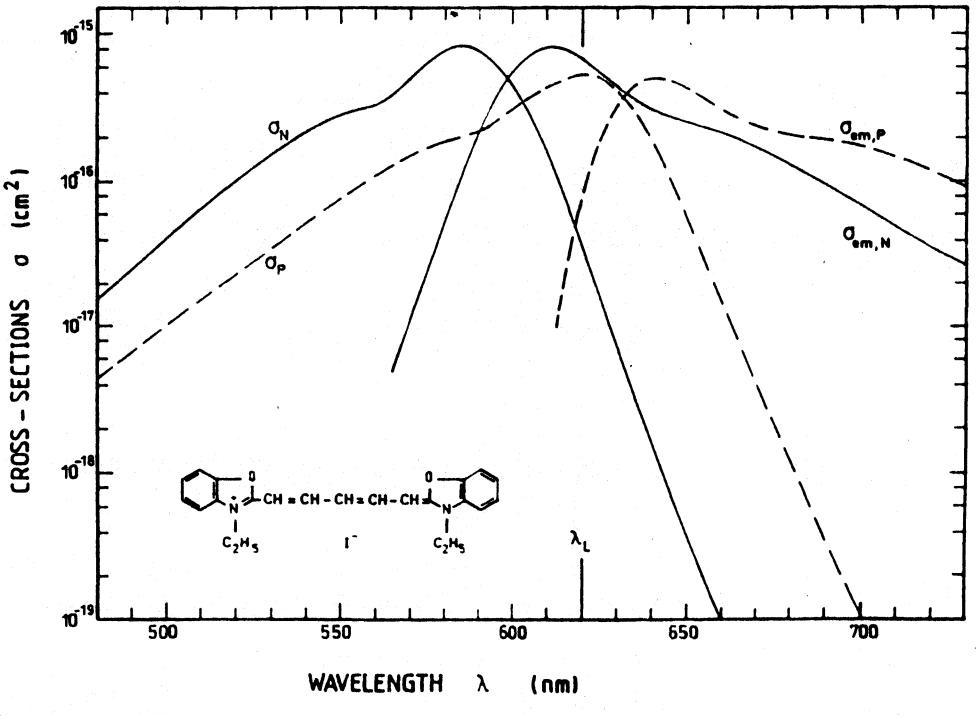

Fig.1: Apparent absorption and emission cross-section spectra of N- and P-isomers of DODCI in ethylene glycol.

From: Proceedings of the International Conference on Lasers'91, edited by F.J. Duarte and D.G. Harris, (STS Press, McLean, VA.,1992), p.890.

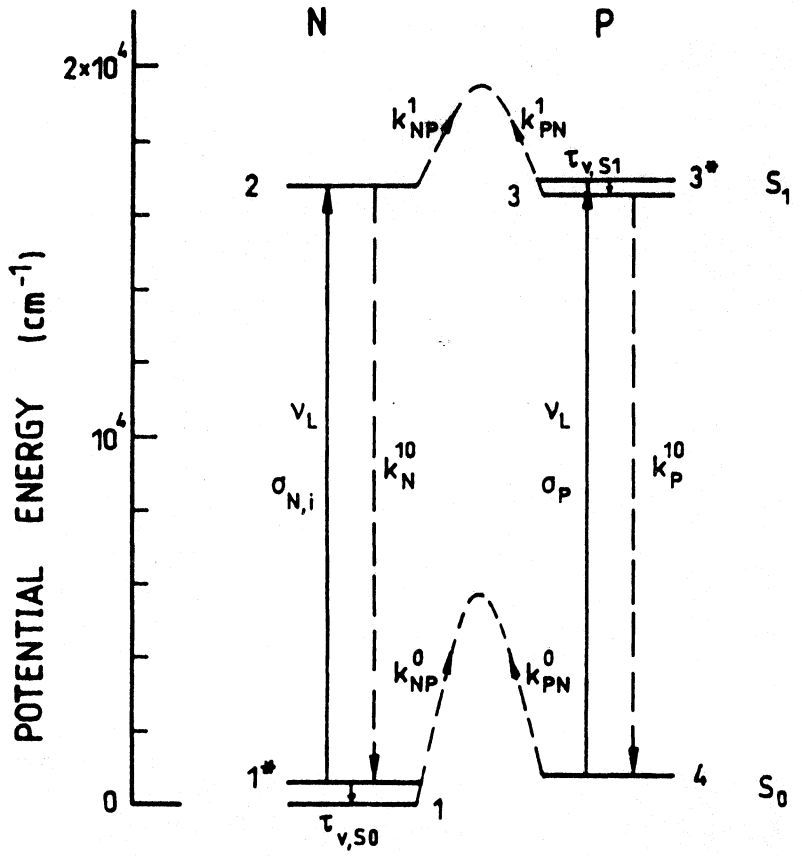

Fig.2: Relevant energy level diagram of DODCI for saturable absorption dynamics.

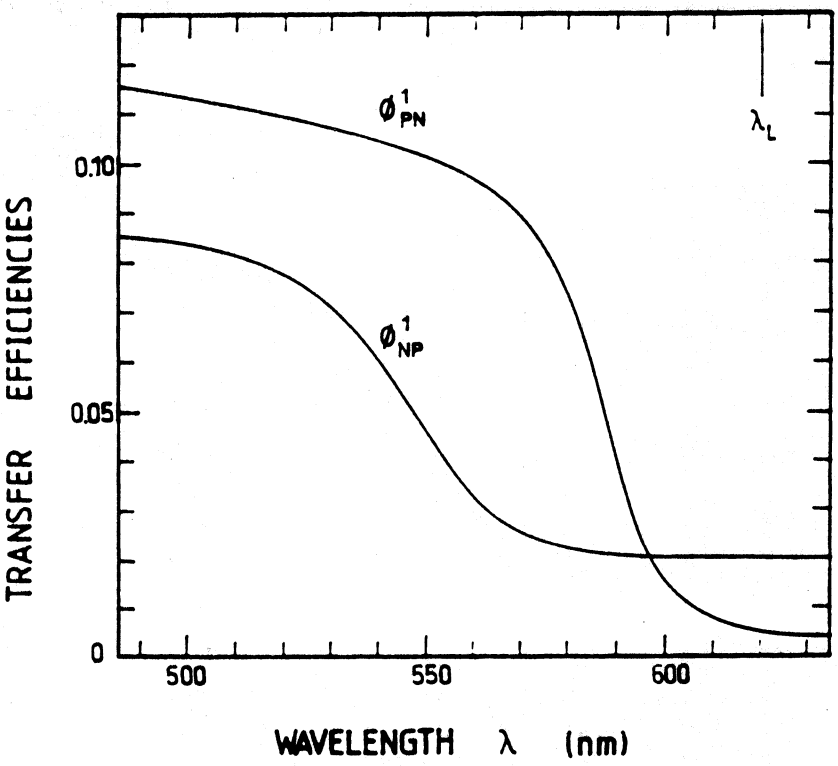

Fig.3: S_1-state N $\rightarrow$ P isomerization transfer efficiency Φ^1_{NP} and P $\rightarrow$ N isomerization transfer efficiency Φ^1_{PN} .

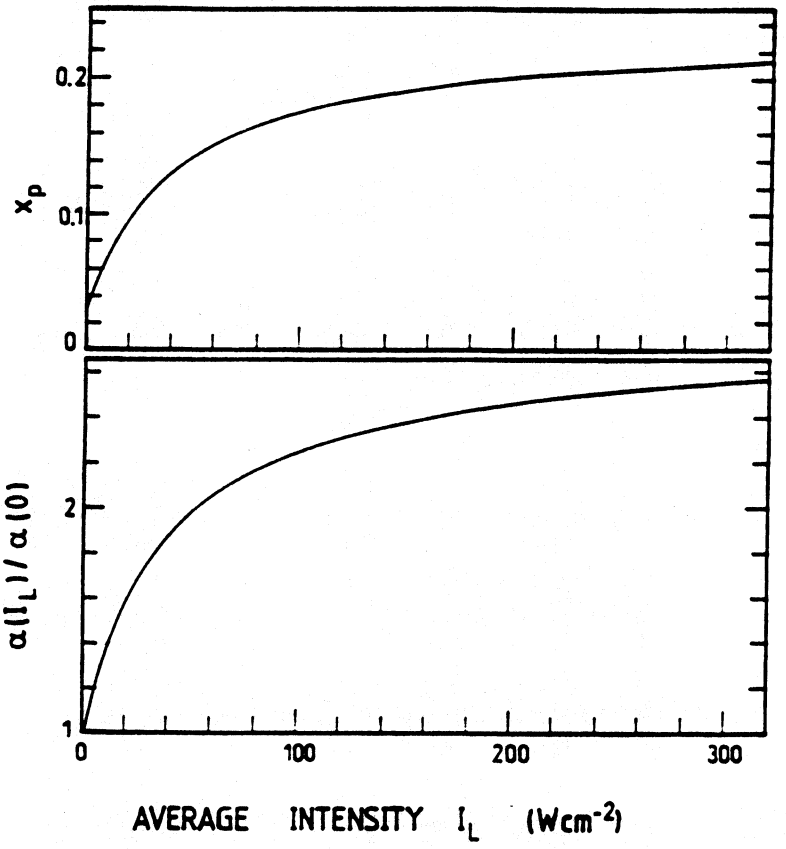

Fig.4: Mole-fraction x_P of P-isomers and absorption increase, $\alpha(I_L)/\alpha(0)$, versus excitation laser intensity I_L at $\lambda_L = 620nm$.

Table 1: Spectroscopic data of DODCI in ethylene glycol at room temperature. Wavelength $\lambda_L = 620nm$

Parameter	Value	Reference
ρ_N	0.06	15
$\sigma_{N,i}$ (cm^2)	7×10^{-16}	11
$\tau_N = k_{N,tot}^{-1}$ (ns)	1.3	11
k_N^{10} (s^{-1})	1.54×10^7	12
k_{NP}^1 (s^{-1})	7.54×10^8	12
k_{NP}^0 (s^{-1})	15	19
$\tau_{v,S0}$ (ps)	1	assumed
$I_{S,ss,N}$ (Wcm^{-2})	3.5×10^5	Eq.10
σ_P (cm^2)	5.2×10^{-16}	11
$\tau_P = k_{P,tot}^{-1}$ (ns)	1.4	11
k_P^{10} (s^{-1})	3.57×10^6	12
k_{PN}^1 (s^{-1})	7.11×10^8	12
k_{PN}^0 (s^{-1})	465	12
$\tau_{v,S1}$ (ps)	0.95	20
$I_{S,ss,P}$ (Wcm^{-2})	4.4×10^5	Eq.10

relative to the N-isomer[10,11], and the separation of the apparent N-isomer and P-isomer absorption cross-section spectra [10,11]. The separated spectra are shown in Fig.1.

Temperature dependent fluorescence quantum distribution measurements allowed to determine the S_1-state level positions of the N- and P-isomers and the S_1-state activation energies for the N $\leftrightarrow$ P photoisomerization[11]. The obtained stimulated emission cross-section spectra of the N- and P-isomers are included in Fig.1. The S_0 and S_1 level positions and barrier heights[11,12] are shown in Fig.2. The obtained fluorescence lifetimes τ_N and τ_P are listed in Table 1.

The photoinduced wavelength dependent N-isomer $\rightarrow$ P-isomer (transfer rate k_{NP}^1 , transfer efficiency $\Phi_{NP}^1 = k_{NP}^1 / k_{N,tot}$, $k_{N,tot} = k_{NP}^1 + k_N^{10}$) and P-isomer $\rightarrow$ N-isomer (k_{PN}^1 , $\Phi_{PN}^1 = k_{PN}^1 / k_{P,tot}$) isomerization rates were determined by laser induced P-isomer accumulation studies[12]. The transfer efficiencies are shown in Fig.3.

The steady-state P-isomer accumulation in the S_0-state is determined by the laser light intensity, the wavelength dependent absorption cross-sections σ_N and σ_P, and the wavelength dependent transfer efficiences Φ^1_{NP} and Φ^1_{PN} . In Fig.4, the P-isomer mole-fraction x_P and the increase of the absorption coefficient α at the wavelength $\lambda_L = 620nm$ (wavelength of cw pumped passive mode-locked femtosecond rhodamine 6G - DODCI laser) is displayed versus the steady-state laser intensity (time averaged intensity of mode-locked laser).

3. Saturable Absorption Dynamics

In the following the nonlinear transmission studies through a DODCI sample are restricted to an excitation wavelength of $\lambda_L = 620nm$. The relevant level system and the transition channels are shown in Fig.2[13]. The spectroscopic parameters involved are given in Table 1.

The N-isomer absorption at $\lambda_L = 620nm$ is governed by the $1, 1^*, 2$ - three-level system. The absorption starts from the Franck-Condon level 1^* in the S_0-state. Only a small fraction ρ_N of thermally excited molecules in the S_0-state takes part in the absorption. The absorption cross-section of the interacting molecules is $\sigma_{N,i} = \sigma_{em,N}$ (see Fig.1)[14] . The transition terminates at the potential energy minimum of the S_1-state. The absorption recovery occurs due to a fast refilling of the level 1^* by molecules in the S_0-state (fast partial absorption recovery time, S_0-state intraband relaxation time $\tau_{v,S0}$, S_0-state spectral cross-relaxation time) and due to a slow $S_1 - S_0$ interband relaxation (relaxation rate k^{10}_N, slow final absorption recovery).

The P-isomer absorption at $\lambda_L = 620nm$ is characterized by the $4, 3^*, 3$ - three-level system. The $S_0 - S_1$ light absorption terminates in the S_1-state Franck-Condon level 3^*. From there a fast relaxation occurs to the relaxed S_1-state level 3 (fast partial absorption recovery time, S_1-state intraband relaxation time $\tau_{v,S1}$, Franck-Condon relaxation time). The refilling of the S_0-ground state occurs with a rate constant k^{10}_P (slow final absorption recovery).

The N-isomer and P-isomer three-level systems are coupled by the isomerization transfer rates. The absorption dynamics is described by the following differential equation system[13,15]. The absorption anisotropy caused by the electric dipole interaction is neglected. The equation system for the number densities N_i of the level populations and for the laser intensity I_L read:

$$\frac{\partial N_1}{\partial t'} = -\frac{\sigma_{N,i}}{h\nu_L}(N_{1^*} - N_2)I_L + k^{10}_N N_2 + k^0_{PN} N_4 - k^0_{NP} N_1 \tag{1}$$

$$\frac{\partial N_{1^*}}{\partial t'} = -\frac{\sigma_{N,i}}{h\nu_L}(N_{1^*} - N_2)I_L - \frac{N_{1^*} - \rho_N N_1}{\tau_{v,S0}} \tag{2}$$

$$\frac{\partial N_2}{\partial t'} = \frac{\sigma_{N,i}}{h\nu_L}(N_{1^*} - N_2)I_L + k^1_{PN}(N_3 + N_{3^*}) - k_{N,tot} N_2 \tag{3}$$

$$\frac{\partial N_3}{\partial t'} = \frac{N_{3^*}}{\tau_{v,S1}} + k^1_{NP} N_2 \frac{N_3}{N_3 + N_{3^*}} - k_{P,tot} N_3 \tag{4}$$

$$\frac{\partial N_{3^*}}{\partial t'} = \frac{\sigma_P}{h\nu_L}(N_4 - N_{3^*})I_L - \frac{N_{3^*}}{\tau_{v,S1}} + k^1_{NP} N_2 \frac{N_{3^*}}{N_3 + N_{3^*}} - k_{P,tot} N_{3^*} \tag{5}$$

$$\frac{\partial N_4}{\partial t'} = -\frac{\sigma_P}{h\nu_L}(N_4 - N_{3^*})I_L + k^{10}_P(N_3 + N_{3^*}) + k^0_{NP} N_1 - k^0_{PN} N_4 \tag{6}$$

$$\frac{\partial I_L}{\partial z'} = -I_L[\sigma_{N,i}(N_{1^*} - N_2) + \sigma_P(N_4 - N_{3^*})] \tag{7}$$

N_1 is the total N-isomer S_0 -state population. It includes N_{1^*}. The initial level populations are $N_1(t' = -\infty, z) = (1 - x_P)N_A$, $N_{1^*}(t' = -\infty, z) = (1 - x_P)\rho_N N_A$, $N_2(t' = -\infty, z) = N_3(t' = -\infty, z) = N_{3^*}(t' = -\infty, z) = 0$, and $N_4(t' = -\infty, z) = x_P N_A$, where N_A is the total number density of DODCI molecules. The intensity transmission through a DODCI sample of length ℓ_A is $T_I = I_L(\ell_A)/I_L(0)$. The time-integrated transmission is

$$T_{TI} = \frac{\int_{-\infty}^{\infty} I_L(t', \ell_A)\, dt'}{\int_{-\infty}^{\infty} I_L(t', 0)\, dt'} \tag{8}$$

The small-signal transmission is

$$T_0 = exp\{-[(1 - x_P)\rho_N \sigma_{N,i} + x_P \sigma_P] N_A \ell_A\} \tag{9}$$

If the isomerization transfer rates are neglected, both the N-isomer and the P-isomer absorption dynamics is characterized by a three-level system with fast partial absorption recovery time τ_{rec} $(= \tau_{v,S0}, \tau_{v,S1})$ and a slow final absorption recovery time τ_A $(= 1/k^{10}_N, 1/k^{10}_P$, or $\tau_N = 1/k_{N,tot}, \tau_P = 1/k_{P,tot}$). The steady-state saturation intensity $I_{S,ss}$ (pulse duration $\Delta t_L \gg \tau_A$), where the absorption coefficient α has reduced to half of its small-signal value, is given by[16]

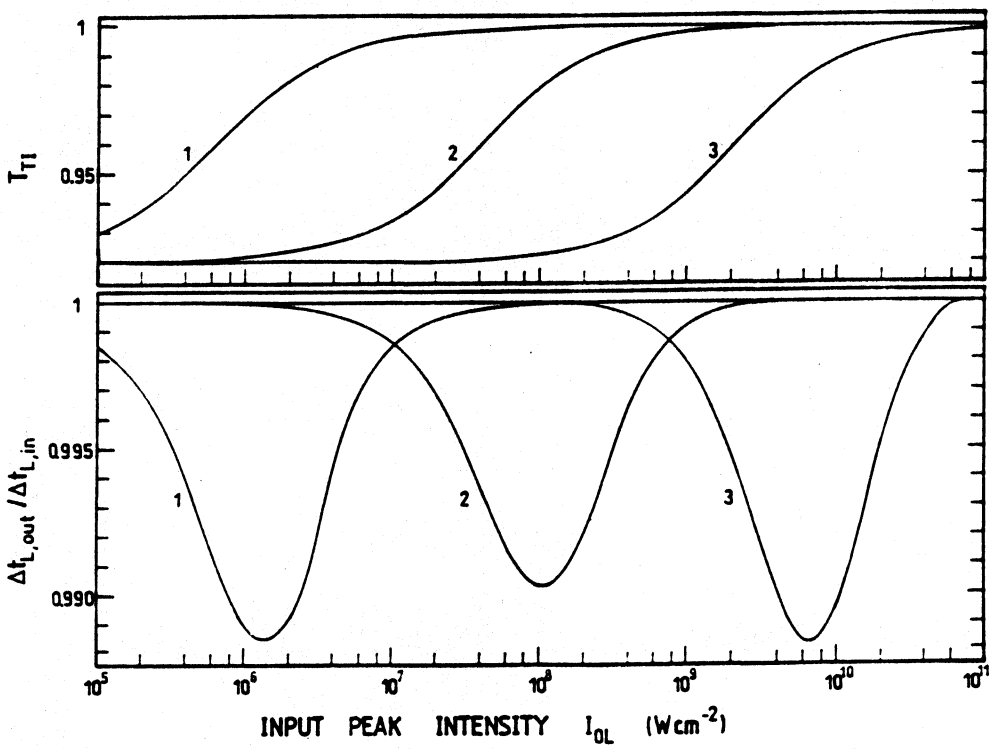

Fig.5: Time-integrated transmission T_{TI} and pulse-shortening ratio, $\Delta t_{L,out}/\Delta t_{L,in}$, versus input peak intensity I_{0L}. Gaussian input pulses of duration (1) $\Delta t_{L,in} = 1ns$, (2) $10ps$, and (3) $100fs$.

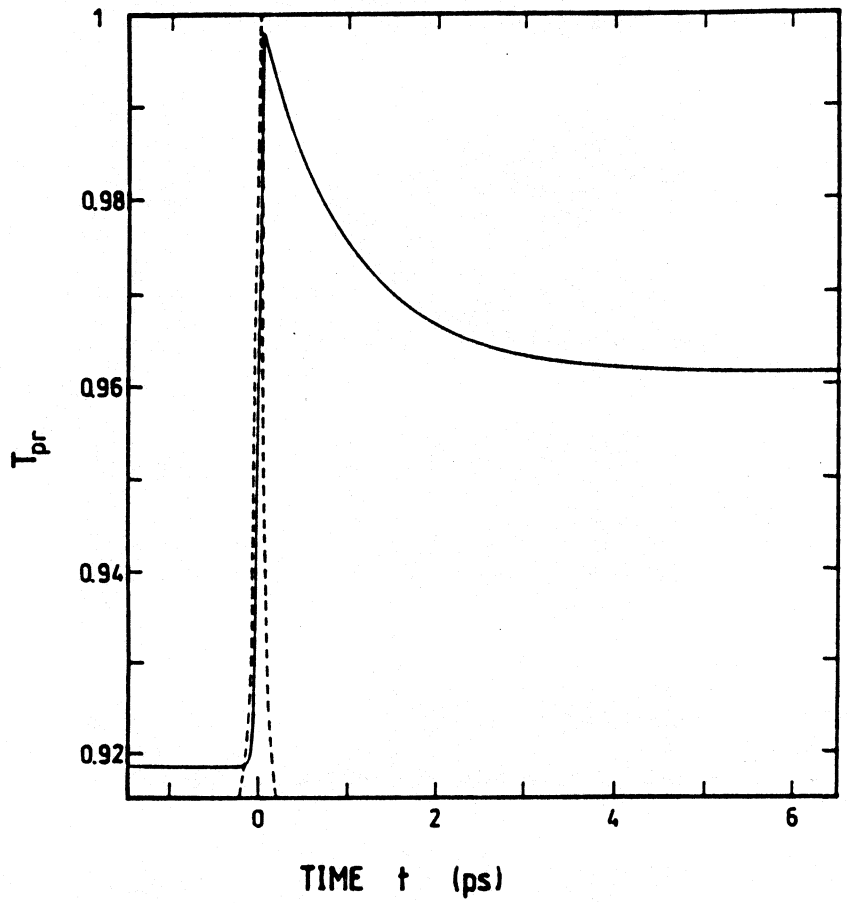

Fig.6: Small-signal probe pulse transmission versus time. Dashed curve shows pump pulse shape.

$$I_{S,ss} = \frac{h\nu_L}{\kappa\sigma\tau_A} \tag{10}$$

where κ is a value between 1 and 2. For $\tau_{rec} \ll \tau_A$ (two-level system with fast intermediate state) it is $\kappa = 1$, and for $\tau_{rec} \gg \tau_A$ (two-level system) it is $\kappa = 2$. In both cases the slow final absorption recovery time determines the steady-state saturation intensity. DODCI has a high absorption cross-section and a slow final absorption recovery time, therefore $I_{S,ss}$ is small (see Table 1) and the mode-locking threshold intensity is low which facilitates cw pumped passive mode-locking.

The transient saturation intensity $I_{S,tr}$ (pulse duration $\Delta t_L \ll \tau_A$) is inverse proportional to the pulse duration. It may be defined as

$$I_{S,tr} = \frac{h\nu_L}{\kappa\sigma\Delta t_L} \tag{11}$$

In Fig.5a the time-integrated transmission T_{TI} is plotted versus input peak intensity I_{0L} of Gaussian pulses of different duration Δt_L. The absorber parameters apply to typical data used in the absorber jet of a femtosecond laser ($N_A = 2.6 \times 10^{17} cm^{-3}, \ell_A = 35\mu m, T_{0,th} = 0.95$, $x_{P,th} = x_P(I_L = 0) = 0.029$, and $x_P = 0.1$, see Fig.4). The pulse shortening ratio, $\Delta t_{L,out}/\Delta t_{L,in}$, of a Gaussian pulse in a single passage through the saturable absorber is shown in Fig.5b. The same parameters apply as in Fig.5a.

The background suppression effect of the fast partial absorption recovery time τ_{rec} is illustrated in Fig.6, where the small-signal probe pulse transmission T_{pr} induced by an intense pump pulse ($\Delta t_L = 0.1ps, I_{0L} = 6.5 \times 10^9 W cm^{-2}$) versus time is plotted. The dye sample parameters are the same as in Fig.5. The partial decrease of the transmission behind the bleaching pulse is responsible for reducing the background signal following the pulse. The background signal is inherently present in the pulse formation process of a passive mode-locked femtosecond dye laser because of the statistical nature of the spontaneous emission which starts the laser action. It is shown in Refs.13 and 15 that without background suppression by the fast partial absorption recovery the formation of stable continuous femtosecond pulse trains does not succeed.

4. Steady-state Pulse Duration in Femtosecond Dye Lasers

A linear passive mode-locked femtosecond dye laser with a prism pair for group velocity dispersion compensation is sketched in Fig.7[17]. The steady-state pulse duration $\Delta t_{L,ss}$ obtained in the laser is determined by a balance between pulse broadening and pulse shortening.

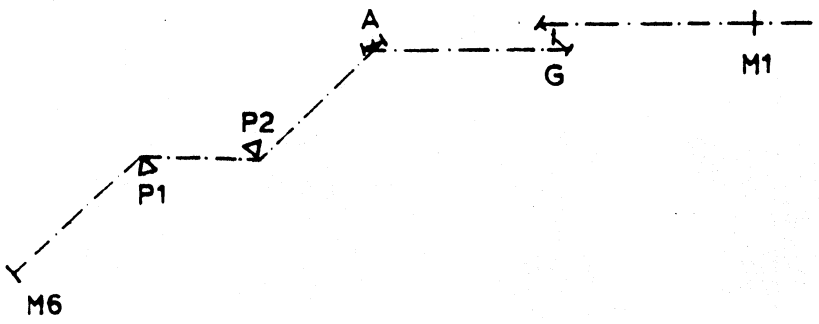

Fig.7: Femtosecond laser arrangement. M1, output mirror. M6, front mirror. A, absorber cavity. G, gain cavity.

Without the prism pair in the resonator, pulse broadening occurs mainly because of the positive group velocity dispersion (GVD) caused by the normalous refractive index dispersion of ethylene glycol in the gain and absorber jet. The GVD is enhanced by the positive self-phase modulation (SPM) caused by the optical Kerr effect in the gain and absorber jet (ethylene glycol). The pulse shortening is achieved by the saturable absorber action. For a typical experimental situation (for parameters see Ref.15) the pulse broadening and pulse shortening per resonator round-trip are displayed in Fig.8. The steady-state pulse duration $\Delta t_{L,ss}$ is given by the crossing point of the pulse broadening and pulse shortening curve (= 150 fs in Fig.8).

Shorter pulse durations may be obtained by reducing the GVD[17,18]. This may be achieved by proper adjustment the prism positions. A schematic dependence of the steady-state pulse duration $\Delta t_{L,ss}$ and of the steady state spectral pulse width $\Delta\nu_{L,ss}$ on the GVD (expressed by $\partial t_{tr}/\partial\nu$, t_{tr} is the transit time broadening, ν is the frequency) is shown in Fig.9. With decreasing positive GVD, $\Delta t_{L,ss}$ shortens and $\Delta\nu_{L,ss}$ broadens. On the right side of position a, the pulse broadening by positive GVD is compensated by the pulse shortening action of the saturable absorber (absorber balanced regime). In the region between a and b, the laser action is self-quenched (repetitive self-termination) since the steady state spectral width $\Delta\nu_{L,ss}$ becomes broader than the spectral amplification width of the gain medium, and the pulse shortening causes the laser to fall below the laser threshold. Beyond b the negative GVD increases and the steady state pulse duration increases. In this negative GVD regime self-stabilized soliton-like pulse generation occurs. Position b determines the prism-pair balanced position where the shortest femtosecond light pulses under stable operation conditions are generated.

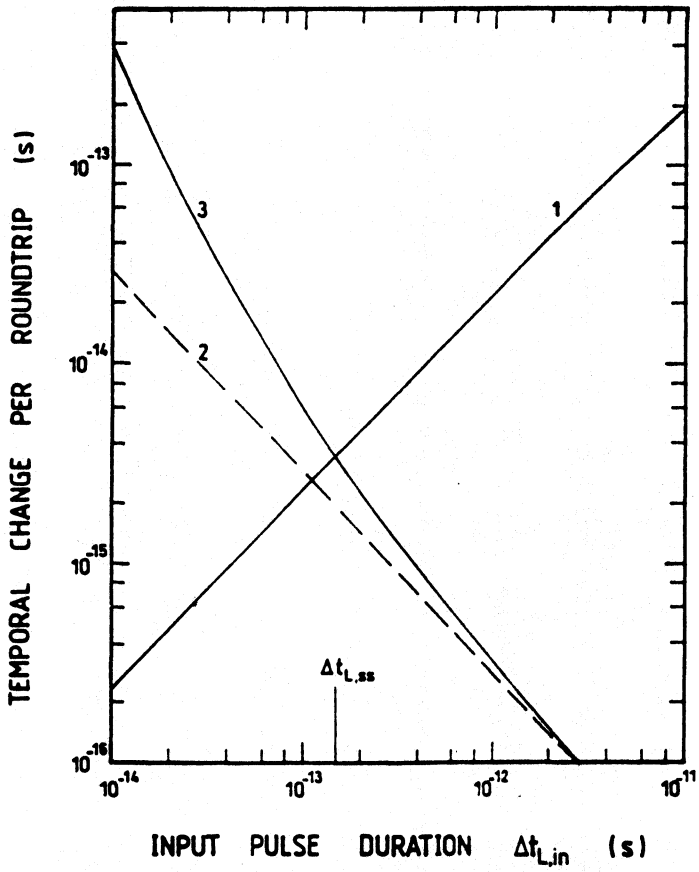

Fig.8: Temporal changes of Gaussian pulses per resonator roundtrip (for data see Ref.15). 1, pulse shortening of saturable absorber. 2, GVD broadening of gain and absorber jet without self-phase modulation (SPM). 3, GVD broadening including effect of SPM.

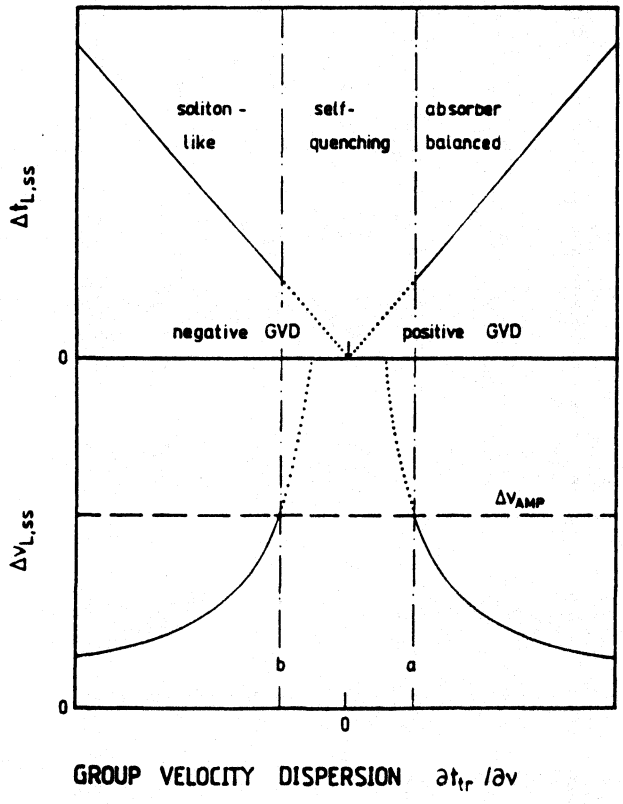

Fig.9: Schematic influence of GVD on steady-state pulse duration $\Delta t_{L,ss}$ and steady-state spectral width $\Delta \nu_{L,ss}$ of passive mode-locked femtosecond laser.

5. Conclusions

DODCI is a good saturable absorber for passive mode-locking of rhodamine 6G femtosecond dye lasers because it has a high absorption cross-section ($\sigma \approx 6 \times 10^{-16} cm^2$) at the laser wavelength and a slow final absorption recovery time ($\tau_A \approx 1.3ns$). These facts give a low mode-locking threshold. In the pulse formation buildup process the P-isomer accumulation reduces the small-signal transmission at the laser frequency and thereby enhances the steady-state pulse shortening action of the dye. The intraband fast partial absorption recovery time τ_{rec} is of the order of 1 ps and is necessary for the background suppression in the transient femtosecond pulse generation process. In femtosecond lasers without compensation of the group velocity dispersion, the steady-state pulse duration is determined by a balance of the pulse shortening action of the saturable absorber DODCI and the pulse broadening action of the positive group velocity dispersion enhanced by positive self-phase modulation. By proper prism pair adjustment to the negative GVD regime, self-stabilized soliton-like short femtosecond pulse generation is achieved[17,18].

References

1. D. N. Dempster, T. Morrow, R. Rankin, and G. F. Thompson, J. Chem. Soc. Faraday Trans. II 68, 1479 (1972).
2. G. R. Fleming, A. E. W. Knight, J. M. Morris, R. J. Robbins, and G. W. Robinson, Chem. Phys. Letters 49, 1 (1977).
3. W. Schmidt and F. P. Schäfer, Phys. Letters A 26, 556 (1968).
4. G. R. Fleming, Chemical Applications of Ultrafast Spectroscopy (Oxford University Press, Oxford, 1986).
5. P. M. W. French, J. A. R. Williams, and J. R. Taylor, Revue Phys. Appl. 22, 1651 (1987).
6. A. Penzkofer, Appl. Phys. B 46, 43 (1988).
7. J. C. Diels, in Dye Laser Principles with Applications, F. J. Duarte and L. W. Hillman, Eds. (Academic Press, Boston, 1990) pp. 41-132.
8. A. Finch, G. Chen, W. Sleat, and W. Sibbett, J. Mod. Opt. 35, 345 (1988).
9. Y. Liu, S. de Silvestri, V. Magni, P. Laporta, and O. Svelto, Acta Opt. Sinica 11, 84 (1991).
10. W. Bäumler and A. Penzkofer, Chem. Phys. Letters 150, 315 (1988).
11. W. Bäumler and A. Penzkofer, Chem. Phys. 140, 75 (1990).
12. W. Bäumler and A. Penzkofer, Chem. Phys. 142, 431 (1990).
13. A. Penzkofer and W. Bäumler, Opt. Quant. Electron. 23, 439 (1991).
14. A. Penzkofer and P. Sperber, Chem. Phys. 88, 309 (1984).
15. A. Penzkofer and W. Bäumler, Opt. Quant. Electron. 23, 727 (1991).
16. M. Hercher, Appl. Optics 6, 947 (1967).
17. W. Bäumler and A. Penzkofer, Opt. Quant. Electron. to be published.
18. O. E. Martinez, R. L. Fork, and J. P. Gordon, J. Opt. Soc. B2, 1985 (1985).
19. J. Jaraudias, J. Photochem. 13, 35 (1980).
20. G. Angel, R. Gagel, and A. Laubereau, Chem. Phys. 131, 129 (1989).